Global Change Biology (2003) **9,** 697–717

MuSICA, a CO_2, water and energy multilayer, multileaf pine forest model: evaluation from hourly to yearly time scales and sensitivity analysis

J. OGÉE*, Y. BRUNET*, D. LOUSTAU†, P. BERBIGIER* and S. DELZON†
Unité de Bioclimatologie – INRA, BP 81, 33883 Villenave d'Ornon Cedex, France, †Unité de Recherches Forestières – INRA, 33610 Pierroton Cedex, France

Abstract

The current emphasis on global climate studies has led the scientific community to set up a number of sites for measuring long-term biospheric fluxes, and to develop a wide range of biosphere–atmosphere exchange models. This paper presents a new model of this type, which has been developed for a pine forest canopy. In most coniferous species the canopy layer is well separated from the understorey and several cohorts of needles coexist. It was therefore found necessary to distinguish several vegetation layers and, in each layer, several leaf classes defined not only by their light regime and wetness status but also by their age. This model, named *MuSICA*, is a multilayer, multileaf process-based model. Each submodel is first independently parameterized using data collected at a EUROFLUX site near Bordeaux (Southwestern France). Particular care is brought to identify the seasonal variations in the various physiological parameters. The full model is then evaluated using a two-year long data set, split up into 12 day-type classes defined by the season, the weather type and the soil water status. Beyond the good overall agreement obtained between measured and modelled values at various time scales, several points of further improvement are identified. They concern the seasonal variations in the stomatal response of needles and the soil/litter respiration, as well as their interaction with soil or litter moisture. A sensitivity analysis to some of the model features (in-canopy turbulent transfer scheme, leaf age classes, water retention, distinction between shaded and sunlit leaves, number of layers) is finally performed in order to evaluate whether significant simplifications can be brought to such a model with little loss in its predictive quality. The distinction between several leaf classes is crucial if one is to compute biospheric fluxes accurately. It is also evidenced that accounting for in-canopy turbulent transfer leads to better estimates of the sensible heat flux.

Nomenclature

A = Net photosynthesis rate ($\mu mol\,m^{-2}\,s^{-1}$)
$A_{dry,shd,\alpha,j}$ = Net photosynthesis rate of a dry shaded needle of age Y_α ($\mu mol\,m^{-2}\,s^{-1}$)
$A_{dry,sun,\alpha,j}$ = Net photosynthesis rate of a dry sunlit needle of age Y_α ($\mu mol\,m^{-2}\,s^{-1}$)
$A_{wet,shd,\alpha,j}$ = Net photosynthesis rate of a wet shaded needle of age Y_α ($\mu mol\,m^{-2}\,s^{-1}$)
$A_{wet,sun,\alpha,j}$ = Net photosynthesis rate of a wet sunlit needle of age Y_α ($\mu mol\,m^{-2}\,s^{-1}$)
C_a ($C_{a,j}$ or $C_{a,r}$) = Air CO_2 concentration (at level z_j or z_r) ($\mu mol\,m^{-3}$)
C_s = Air CO_2 concentration at leaf surface ($\mu mol\,m^{-3}$)
$\tilde{d}^f_{ij}$ ($\tilde{d}^n_{ij}$) = Far-field (near-filed) neutral normalized dispersion matrix ($s\,m^{-1}$)
D_0 = Parameter for the stomatal conductance model (hPa)
D_s = Air vapour pressure deficit in leaf boundary-layer (hPa)
D_{ij} = Dispersion matrix for turbulent transfer ($s\,m^{-1}$)
E = Water vapour flux at reference level z_r ($kg\,m^{-2}$)

Correspondence: Jérôme Ogée, LSCE – CEA/CNRS, Orme des Merisiers, 91191 Gif/Yvette Cedex, France, tel. +33(0) 1 69 08 87 27, fax +33(0) 1 69 08 77 16, e-mail: ogee@lsce.saclay.cea.fr

$F_{c,0}$ = Forest floor CO_2 efflux ($\mu mol\,m^{-2}\,s^{-1}$)
g_0 = Parameter for the stomatal conductance model ($mmol\,m^{-2}\,s^{-1}$)
g_s = Stomatal conductance ($mmol\,m^{-2}\,s^{-1}$)
h = Canopy height (m)
J_m = Potential electron transport rate ($\mu mol\,m^{-2}\,s^{-1}$)
K_f = Far-field diffusivity ($m^2\,s^{-1}$)
L = Obukhov length scale (m)
$L_{c,tot}$ = Canopy leaf area index ($m^2\,m^{-2}$)
L_α = Whole-sided leaf area of all needles of age Y_α ($m^2\,m^{-2}$)
m = Parameter for the stomatal conductance mode (dimensionless)
P_r = Rainfall rate at reference level z_r ($kg\,m^{-2}$)
$P_{sun,\alpha,j}$ = Fraction of sunlit needle sections of age Y_α and at level z_j (dimensionless)
$P_{wet,\alpha,j}$ = Fraction of wet needle sections of age Y_α and at level z_j (dimensionless)
$q_a\,(q_{a,j})$ = Air humidity (at level z_j) ($g\,kg^{-1}$)
$Q_{abs,b,\alpha,j}$ = Direct solar radiation absorbed by a shoot of age Y_α ($W\,m^{-2}$)
$Q_{abs,d,\alpha,j}$ = Diffuse solar radiation absorbed by a shoot of age Y_α ($W\,m^{-2}$)
$Q_{b,j}\,(Q_{b,r})$ = Direct radiation at level z_j (z_r) ($W\,m^{-2}$)
$Q^+_{d,j}\;Q^-_{d,j}$ = Downward (upward) diffuse radiation at level z_j ($W\,m^{-2}$)
$Q^+_{veg,j}$ = Downward thermal radiation emitted by vegetation at level z_j ($W\,m^{-2}$)
$Q_{th,r}$ = Sky thermal radiation at reference level z_r ($W\,m^{-2}$)
$Q^+_{th,j}$ = Downward thermal radiation at level z_j ($W\,m^{-2}$)
$R_{bole,j}$ = Bole respiration at level z_j ($\mu mol\,m^{-2}\,s^{-1}$)
$Road$ = Dark respiration ($\mu mol\,m^{-2}\,s^{-1}$)
$S_{c,j}$ = CO_2 source/sink density at level z_j ($\mu mol\,m^{-3}\,s^{-1}$)
$STAR_\alpha$ = Silhouette-to-total area ratio of a shoot of age Y_α (dimensionless)
t = Time (s)
$T_a\,(T_{a,j})$ = Air temperature (at level z_j) (K)
T_L = Lagrangian time scale (s)
T_{opt} = Optimal temperature for photosynthetic parameters (K)
$U\,(U_j)$ = Wind speed (at level z_j) ($m\,s^{-1}$)
$\tilde{u}_j$ = Neutral normalized wind speed at level z_j (dimensionless)
U^* = Friction velocity ($m\,s^{-1}$)
V_m = Maximum rate of carboxylation ($\mu mol\,m^{-3}\,s^{-1}$)
W_d = Bulk soil water content ($kg\,m^{-2}$)
W_{ref} = Any leaf photosynthetic/respiratory parameter at 25 °C
Y_α = Shoot/needle age (yr)
z_j, z_i = Heights (m)
z_r = Reference height (m)
z^* = Roughness sublayer height (m)
Δz_j = Source/layer thickness (m)
Γ^* = Compensation point for photosynthesis ($\mu mol\,m^{-3}$)
$\Sigma_{sun,\alpha}$ = Fraction of sunlit needle sections in a shoot of age Y_α (dimensionless)
α_j = Quantum efficiency for photosynthesis $(mol(CO_2)\,mol(photons)^{-1})$
ϕ_h = Stability correction function for K_f (dimensionless)
ϕ_m = Stability correction function for horizontal wind speed (dimensionless)
ϕ_w = Stability correction function for σ_w (dimensionless)
γ_U = Proportion of green leaves in the understorey (dimensionless)
κ_b = Extinction coefficient for solar direct radiation (dimensionless)
μ_b = Sine of sun elevation angle (dimensionless)
ν_0 = Parameter for stomatal conductance model (dimensionless)
$\Pi_{b,j}$ = Fraction of direct solar radiation at level z_j (dimensionless)
$\Pi^+_{th,j}$ = Fraction of sky thermal radiation at level z_j (dimensionless)
ρ_c = Reflectance of needles (dimensionless)
σ_w = Standard deviation of vertical wind speed ($m\,s^{-1}$)

τ_c = Transmittance of needles (dimensionless)
ψ_0 = Parameter for stomatal conductance model (MPa)
ψ_b = Soil predawn water potential (MPa)

Keywords: biosphere–atmosphere interaction, ecosystem evaporation, EUROFLUX, FluxNet, maritime pine forest, net ecosystem carbon exchange, soil-vegetation-atmosphere transfer model

Received 15 May 2002; revised version received 28 October 2002 and accepted 14 February 2003

Introduction

The current emphasis on global climate studies has changed our way of considering both measurements and models. Indeed, biosphere–atmosphere exchanges involve a number of processes operating over a broad range of time scales, from seconds (e.g. photosynthesis, turbulence) to weeks (e.g. allocation, acclimation) and years (e.g. mineralization). It has therefore become obvious that surface models, required to evaluate biospheric fluxes for the future, should be able to cope with such a range of scales (Law *et al*., 2000; Baldocchi & Wilson, 2001; Baldocchi *et al*., 2001a; Katul *et al*., 2001; Rasse *et al*., 2001; Wilson *et al*., 2001), and also that long-term flux measurements were necessary to analyze the seasonal behaviour of vegetated surfaces and provide adequate data sets for model validation (Baldocchi *et al*., 2001b; Canadell *et al*., 2000).

In this respect process-based SVAT (Soil-Vegetation-Atmosphere Transfer) models have better potential than more empirical models because they are prone to be valid under a wider range of climate conditions than the range used for model testing. This feature is of particular interest for long-term simulations. However, such simulations can be quite sensitive to the parameterization of processes acting over short time scales (Law *et al*., 2000; Baldocchi & Wilson, 2001; Baldocchi *et al*., 2001a; Wilson *et al*., 2001; Baldocchi *et al*., 2002). Consequently, models used for long-term purposes at a given site should also provide an accurate and consistent representation of instantaneous fluxes at all times of the year. Potentially, the most accurate models are the so-called 'complete' multilayer models (Gu *et al*., 1999), in which the canopy is divided vertically into a finite number of layers, and that calculate the vertical variation in all microclimatic variables (radiation, wind speed, air temperature, concentrations in water vapour and CO_2...). These models allow for an adequate description of the coupling between canopy microclimate and physiological processes such as stomatal function, photosynthesis and respiration. Although they have been mostly developed as research tools to investigate particular processes using relatively short data series (often less than a few weeks), the question of whether they could also be good candidates for long-term simulations and scenario analysis is quite relevant in this research field.

Several multilayer SVAT models are now available in the literature (Baldocchi & Harley, 1995; Leuning *et al*., 1995; Williams *et al*., 1996; Gu *et al*., 1999). Most forest canopy models have been developed for deciduous species. We found it preferable to develop our own model because the present work is part of a research programme on maritime pine (*Pinus pinaster* Ait.), an Atlantic coniferous species covering 4 Mha in Southwest Europe. Indeed, the leaves (needles) of coniferous canopies are clumped in shoots that exhibit strong spatial variability in their shape (Bosc, 2000; Oker-Blom & Smolander, 1988; Cescatti, 1998), age and photosynthetic capacity (Porté & Loustau, 1998; Wang *et al*., 1995). This variability induces noticeable consequences on light interception and radiation use efficiency of the whole canopy (Wang & Jarvis, 1990; Wang & Jarvis, 1993). As most existing models assume intralayer homogeneity it was felt necessary to account for these characteristics, and in particular to distinguish several leaf age classes. In addition, our forest ecosystem is made of two well-separated vegetation layers (understorey and canopy), with a large canopy air space, so that the model has to account for canopy air storage and must distinguish canopy from understorey species.

The resulting model, *MuSICA* (Multi-layer simulator of the interactions between a Coniferous stand and the atmosphere), is a multilayer, multileaf process-based biosphere–atmosphere gas exchange model. A two-year (1997–1998) data set of continuous flux measurements performed at 'Le Bray' site, that has been part of the EUROFLUX network since 1996, is used to evaluate the performance of *MuSICA*.

Until recently, model validations have been performed by comparing either all available instantaneous modelled and measured values, or cumulative values when the data set was long enough. Although such validations are useful since they provide overall quality tests of the model, they have limited potential since they do not give much information on the reasons for the observed discrepancies. The growing availability of long-term

instantaneous flux data sets at more than 100 vegetative sites (Aubinet *et al*., 2000; Baldocchi *et al*., 2001b) offers new possibilities for validation purposes, because they allow the seasonal behaviour of the model to be analyzed under a whole range of environmental conditions. This is what we attempt to do in this paper, in addition to more classical validation procedures, by splitting the two-year data set into 12 classes based on the combination of season, cloud cover, air humidity and soil water status. We show that this makes it easier to evaluate the performances of the model and formulate various modelling hypothesis.

Using complex, multilayer models for long-term investigations may not always be feasible. They require many parameters and may not be, for instance, easily interfaced with Global Circulation Models. The question then naturally arises as to whether simplifications could be brought to the model without causing significant degradation to the overall quality of the results. Simplifications to the model characteristics can affect for example the description of the canopy structure and the number of canopy layers; the distinction between sunlit and shaded leaves, or wet and dry leaves; the need to account for scalar concentration gradients in the canopy air space. It is difficult to address these questions when only a few days worth of measurements are available, since the range of climatic conditions or soil water status is inevitably small. We therefore found it sensible to take advantage of the present modelling exercise to investigate the adequacy of some possible simplification schemes.

This paper is organized as follows. Firstly we briefly describe the *MuSICA* model. Secondly we show how the various submodels were parameterized from independent eco-physiological and micrometeorological measurements. We then present a comparison of modelled and measured biospheric fluxes at various time scales. Finally the sensitivity of the model to various simplifications is analyzed.

Model description

Vegetation representation

As mentioned above *MuSICA* is a multilayer, multileaf process-based biosphere–atmosphere gas exchange model. In each layer several classes of plant parts are distinguished according to their water status (wet or dry leaves in the understorey and the canopy), light regime (sunlit or shaded leaves in the understorey and the canopy) and age (0, 1 or 2-year-old-shoots in the canopy, since maritime pine needles have a lifetime of about three years). In other words, a canopy layer displays 12 'big shoots' and the understorey layer 4 'big leaves'. The model is one-dimensional because all trees have the same age and similar crown depth and height (Berbigier *et al*., 2001). An extensive description of *MuSICA* can be found in Ogée (2000). We give here its main characteristics (see also Table 1).

Radiative transfer model

The radiative microclimate of each 'big leaf' or 'big shoot' is given by incident (upward and downward) photosynthetically active radiation (PAR), incident near-infrared radiation (NIR) and incident thermal infrared radiation (TIR). At any level within the stand PAR and NIR are split up into direct and diffuse components.

One difficulty is to distribute the radiation absorbed by each canopy layer between big shoots of different ages. For this purpose we use the concept of silhouette-to-total area ratio (*STAR*, Oker-Blom & Smolander, 1988; Bosc, 2000). A shoot of age Y_α located at level z_j in the canopy and with silhouette-to-total area ratio $STAR_\alpha$ absorbs direct and diffuse solar radiation ($Q_{abs,b,\alpha,j}$ and $Q_{abs,d,\alpha,j}$, respectively) according to:

$$Q_{abs,b,\alpha,j} = STAR_\alpha \quad Q_{b,r}/\mu_b \times (1 - \rho_c - \tau_c) \quad \text{for direct radiation} \tag{1a}$$

$$Q_{abs,d,\alpha,j} = 2\,STAR_\alpha \quad \left(Q^+_{d,j} + Q^-_{d,j}\right) \times (1 - \rho_c - \tau_c) \quad \text{for diffuse radiation} \tag{1b}$$

where $Q_{b,r}$ is the incident direct solar radiation (PAR or NIR) at a reference level z_r above the canopy and μ_b is the sine of the sun elevation angle, $Q^+_{d,j}$ and $Q^-_{d,j}$ are the incident downward and upward diffuse solar radiation at level z_j and ρ_c and τ_c are the needle reflectance and transmittance (for PAR or NIR), respectively. Throughout the paper index α refers to needle age.

In these expressions we assume that ρ_c and τ_c are equal for all needles and use PAR and NIR values measured by Berbigier & Bonnefond (1995) for maritime pine. We also assume that *STAR* only depends on shoot age. In particular we do not account for any variation with height or projection angle, because our 'big shoots' represent an ensemble average of several shoots whose twigs have different inclination angles. Assuming that the inclination angle distribution is close to the spherical distribution at all heights within the crown we obtain Eqns (1a) and (1b). However it was found necessary to account for variations of *STAR* with shoot age (Bosc, 2000). The procedure is described in the parameterization section.

In order to compute $Q^+_{d,j}$ and $Q^-_{d,j}$ within the canopy we use a two-stream radiative transfer model (Sellers, 1985). Such a model has been successfully tested at our site against global radiation and PAR measurements performed just above the understorey (Berbigier & Bonnefond, 1995; Hassika *et al*., 1997). Short-wave global

Table 1 General features of the *MuSICA* model

SVAT process	Strategy	Key reference
Radiative transfer	Direct, diffuse and upward and downward scattered radiation are treated separately	Berbigier & Bonnefond (1995)
	Scattering within shoots and needles is accounted for when computing the surface area of sunlit needle sections	Bosc (2000)
Turbulent transfer	Scalar transport is treated as either diffusive (far-field) or non-diffusive (near-filed) assuming steady weakly inhomogeneous turbulence	Raupach (1989b)
	Momentum transport is treated as steady and dependent on plant area density and degree of clumping	Massman & Weil (1999)
Rain interception	Vegetation interception factor and storage capacity are taken proportional to leaf area	Bouten *et al*. (1996)
Photosynthesis	Biochemical model expressing photosynthesis rate limited either by RuBP regeneration or by RuBISCO kinetics	Farquhar *et al*. (1980)
Stomatal conductance	Phenomenological model using the linear dependency of stomatal aperture towards net photosynthesis	Leuning (1995)
Boundary-layer conductance	Drag coefficient is computed assuming turbulent flow and forced or free convection	Nikolov *et al*. (1995)
Drought	Stomatal aperture is reduced by an empirical factor depending on soil water content	Nikolov *et al*. (1995)
Soil heat and moisture transfer	Litter is treated as a separate and insulating medium from the soil underneath	Ogée & Brunet (2002)
Soil respiration	Soil respiration is assumed to depend on soil surface temperature only	Loustau *et al*. (2003)

radiation at the reference level is decomposed into direct and diffuse components following Bristow *et al*. (1986) and split up into PAR and NIR components as $1\,\mathrm{W\,m^{-2}}$ of global radiation is equivalent to $2.02\,\mu\mathrm{mol\,m^{-2}\,s^{-1}}$ of PAR (Hassika *et al*., 1997). Understorey albedos for PAR and NIR and diffuse and direct radiation are distinguished (Sellers, 1985).

The projected canopy leaf area index ($L_{c,\mathrm{tot}}$) and the extinction coefficient for direct radiation (κ_b) are computed from the whole-sided leaf areas (L_α) and the silhouette-to-total area ratios ($STAR_\alpha$) of each cohort of needles according to:

$$L_{c,\mathrm{tot}} = \frac{1}{2}\sum_\alpha L_\alpha = \frac{1}{2}\sum_\alpha \int_0^h \ell_\alpha(z)\,\mathrm{d}z \tag{2a}$$

$$\kappa_b\, L_{c,\mathrm{tot}} = \sum_\alpha STAR_\alpha\, L_\alpha \tag{2b}$$

where $\ell_\alpha(z)$ represents the whole-sided leaf area density of needles of age Y_α and h is canopy height. The 1/2 factor is needed to convert whole-sided to projected leaf areas (Chen & Black, 1992). In fact, Eqn (2b) is applied to each canopy layer so that direct radiation attenuates within the canopy according to:

$$\begin{aligned} Q_{b,j} &= Q_{b,r}\exp\left(-\sum_\alpha STAR_\alpha/\mu_b \int_{z_j}^h \mathrm{d}z'\,\ell_\alpha(z')\right) \\ &= Q_{b,r}\Pi_{b,j} \end{aligned} \tag{3}$$

where $Q_{b,j}$ is the direct radiation at level z_j and $\Pi_{b,j}$ is the penetration function for direct radiation. The penetration function for solar diffuse radiation is computed as in Berbigier & Bonnefond (1995), i.e., with Eqn (3) and assuming a standard overcast sky.

Following Bosc (2000), shoot surface fluxes (CO_2 assimilation, transpiration and sensible heat flux) are computed as the sum of two fluxes corresponding to two needle areas, $\Sigma_{\mathrm{sun},\alpha}$ (with absorbed radiation $Q_{\mathrm{abs,b,j},\alpha}/\Sigma_{\mathrm{sun},\alpha} + Q_{\mathrm{abs,d,j},\alpha}$) and $1-\Sigma_{\mathrm{sun},\alpha}$ (with absorbed radiation $Q_{\mathrm{abs,d,j},\alpha}$). $\Sigma_{\mathrm{sun},\alpha}$ is equal to the area of the needle segments that have a face directly illuminated by the sun, normalized by the total shoot area. We use $\Sigma_{\mathrm{sun},\alpha}$ to account explicitly for shoot clumping and internal rediffusion of the direct beam within the needles (Bosc, 2000).

As for $STAR_\alpha$ we consider in each layer an ensemble average of even-aged shoots so that $\Sigma_{\mathrm{sun},\alpha}$ can be considered independent of height and sun elevation angle. The fraction of sunlit needle segments between levels z_j

and $z_j + \Delta z_j$ within the canopy is then given by the fraction of sunlit shoots multiplied by $\Sigma_{sun,\alpha}$:

$$P_{sun,\alpha,j} = \Sigma_{sun,\alpha} \times \int_{z_j}^{z_j+\Delta z_j} dz \times \exp\left(-\sum_{\alpha} STAR_\alpha/\mu_b \int_{z}^{h} \ell_\alpha(z')\,dz'\right) \quad (4)$$

Downward thermal infrared radiation at level z_j within the canopy is computed as:

$$Q^+_{th,j} = Q^+_{veg,j} \times \left(1 - \Pi^+_{th,j}\right) + Q_{th,r} \times \Pi^+_{th,j} \quad (5)$$

where $Q_{th,r}$ is the sky thermal infrared radiation at reference level and $\Pi^+_{th,j}$ is the penetration function (Berbigier & Bonnefond, 1995). $Q^+_{veg,j}$ represents the downward thermal infrared radiation emitted by vegetation at level z_j: it is a function of the surface temperatures of all needles above z_j with weighting factors depending on $\ell_\alpha(z)$ (Gu *et al*., 1999; Ogée, 2000). Upward thermal infrared radiation within the canopy is computed in a similar way with $Q_{th,r}$ replaced by thermal infrared radiation emitted by the understorey and the ground.

Turbulent transfer model

The non-radiative microclimate of each 'big leaf' and 'big shoot' is given by air temperature (T_a), air mixing ratio (q_a), air CO_2 concentration (C_a) and mean wind speed (U).

In the roughness sublayer the stability parameter is usually considered as constant and equal to h/L (Pereira & Shaw, 1977; Shaw *et al*., 1988; Leclerc & Beissner, 1990; Jacobs *et al*., 1992) or alternatively to z^*/L, where z^* is the roughness sublayer height and L is the Obukhov length scale, computed with above canopy turbulence data. The latter definition is used and the mean wind speed is computed as:

$$U_j = \tilde{u}_j \times U^* \times \phi_m\left(\frac{z^*}{L}\right) \quad (6)$$

where $\tilde{u}_j$ is the neutral wind speed profile normalized by the friction velocity U^* and ϕ_m is the stability correction function for momentum transfer (independent of level z_j). Within the canopy $\tilde{u}_j$ attenuates exponentially (Massman & Weil, 1999) and above the canopy, but still in the roughness sublayer, it is computed according to Cellier & Brunet (1992).

Scalar concentration C_a (alternatively T_a or q_a) at all levels z_i is computed with a Lagrangian turbulent transfer scheme summarized in the equation (Raupach, 1989a):

$$C_{a,i} - C_{a,r} = \sum_j D_{ij}\, S_{c,j}\, \Delta z_j + D_{i0}\, F_{c,0} \quad (7)$$

where $C_{a,r}$ is the CO_2 concentration at the reference level above the canopy, $S_{c,j}$ is the CO_2 source/sink strength of vegetation layer j with thickness Δz_j, $F_{c,0}$ is the forest floor CO_2 efflux and D_{ij} is the turbulent dispersion matrix. The latter depends on turbulence statistics and is computed as a sum of far-field and near-field components according to the localized near-field theory of Raupach (1989b). Stability effects are accounted for as in Leuning (2000), except that we use here a constant stability parameter (z^*/L), which provides the following linear equation:

$$D_{ij} = \frac{\tilde{d}^f_{ij}}{U^*}\phi_h\left(\frac{z^*}{L}\right) + \frac{\tilde{d}^n_{ij}}{U^*}\phi_w^{-1}\left(\frac{z^*}{L}\right) \quad (8)$$

where ϕ_h and ϕ_w are the stability correction functions for the (far-field) scalar turbulent diffusivity (K_f) and the standard deviation of vertical velocity (σ_w), respectively. Matrix elements $\tilde{d}^f_{ij}$ and $\tilde{d}^n_{ij}$ are then independent of the turbulent variables U^* and L; they only depend on the neutral normalized profiles of σ_w and K_f, expressed as a function of canopy structure (see the parameterization section).

Scalar source densities

The CO_2 source/sink density in Eqn (7) is the sum of the CO_2 assimilation rates of all the 'big shoots' or 'big leaves' and the respiration rates of the trunk and branch sections found within this layer. For a layer j with thickness Δz_j within the canopy we write:

$$S_{c,j} = \sum_{\alpha} \int_{\Delta z_j} \gamma_\alpha(z)\,dz \times \left\{(1 - P_{sun,\alpha,j}) \times [(1 - P_{wet,\alpha,j}) \times A_{dry,shd,\alpha,j} + P_{wet,\alpha,j} \times A_{wet,shd,\alpha,j}] + P_{sun,\alpha,j} \times [(1 - P_{wet,\alpha,j}) \times A_{dry,sun,\alpha,j} + P_{wet,\alpha,j} \times A_{wet,sun,\alpha,j}]\right\} + R_{bole,j} \quad (9)$$

$P_{wet,\alpha,j}$ represents the fraction of wet needles of age Y_α within the vegetation layer j. $A_{dry,sun,\alpha,j}$, $A_{dry,shd,\alpha,j}$, $A_{wet,sun,\alpha,j}$ and $A_{wet,shd,\alpha,j}$ are the CO_2 assimilation rates at the surface of needle sections of age Y_α that are, respectively, dry and sunlit, dry and shaded, wet and sunlit and wet and shaded. $R_{bole,j}$ represents the respiration rate of all trunk and branch sections of layer j. In the understorey the expression is simpler because we assume that all leaves belong to a single age class.

Rain interception model

To compute $P_{wet,\alpha,j}$ we use a multilayer rain interception model inspired from Whitehead & Kelliher (1991) and Bouten *et al*. (1996). The evaporation rates within each

layer are given by an equation similar to Eqn (9), the summation being restricted to wet leaves. The fraction of intercepted rain and the maximum storage capacity are assumed proportional to leaf area for each vegetation layer and each cohort of needles (Whitehead & Kelliher, 1991). In our model the CO_2 diffusion pathway at the leaf surface is assumed to be blocked by droplets whenever leaves are wet.

Leaf gas-exchange model

The fluxes (evaporation, transpiration, CO_2 assimilation, sensible heat flux) at the surface of each 'big shoot' or 'big leaf' are computed with a simple leaf model accounting for photosynthesis (Farquhar *et al*., 1980), stomatal conductance (Leuning, 1995), boundary-layer conductance (Landsberg & Powell, 1973; Grant, 1984) and including a leaf energy budget (Gu *et al*., 1999; Paw, 1987). The boundary-layer conductance submodel accounts for clumping of needles and leaves, as was done by Grant (1984) and Landsberg & Powell (1973), respectively. The stomatal conductance submodel is slightly different from that of Leuning (1995): in order to account for soil water stress the stomatal conductance of a leaf (g_s) is multiplied by an empirical function of the soil predawn water potential (ψ_b), following Nikolov *et al*. (1995). This gives:

$$g_s = \left\{ g_0 + \frac{mA}{(C_s - \Gamma^*)(1 + D_s/D_0)} \right\} \times \frac{1}{1 + (\psi_b/\psi_0)^{v_0}} \quad (10)$$

where g_0, m and D_0 are parameters of the stomatal conductance model of Leuning (1995), A is net CO_2 assimilation, D_s and C_s are the air water vapour deficit and the CO_2 concentration in the leaf boundary layer, respectively, Γ^* is the CO_2 compensation point, and ψ_0 and v_0 are adjustable parameters.

Soil/litter gas-exchange model

To compute evaporation and sensible heat flux at the forest floor we used the soil and litter model of Ogée & Brunet (2002) that was successfully tested at our site. Forest floor CO_2 efflux is given by a simple Q_{10}-law depending on the soil–litter interface temperature (Ogée & Brunet, 2002).

Resolution scheme

At the start of each day the information on plant structure and physiological capacity is updated and the normalized profiles of $\tilde{d}^{f}_{ij}$, $\tilde{d}^{n}_{ij}$ and $\tilde{u}_j$ are computed accordingly. At each time step the model first reads the site meteorological data (global and sky thermal radiation, rainfall, wind speed, air pressure, air temperature, air mixing ratio and air CO_2 concentration at z_r). Global radiation is then split up into PAR and NIR, as well as direct and diffuse components, and the short-wave radiation field is solved within the vegetation.

As for turbulent transfer, the model is initialized with the values obtained for L and the scalar gradients at the previous time step. As a first guess leaf surface temperatures are taken equal to the air temperature at the same level. This allows the long-wave radiation field to be computed in the vegetation. Then the leaf gas-exchange fluxes are computed for each 'big shoot' and 'big leaf', thereby leading to new estimates of leaf surface temperatures. A first iteration is performed on these temperatures through the long-wave radiative transfer model. This iterative scheme has already been tested by Su *et al*. (1996). Convergence is achieved when the difference between two iterations, for all long-wave absorbed radiative fluxes, is less than $10^{-2}\,W\,m^{-2}$. This usually takes no more than 4–5 iterations.

From the leaf gas-exchange fluxes of each 'big shoot' and 'big leaf' we are now able to compute the scalar source densities (Eqn (9)) and the corresponding turbulent fluxes. This provides a new estimate of L, used in turn to get updated estimates of the wind speed profile, U^* (Eqn (6)) and the scalar profiles (Eqns (7) and (8)). A new iteration loop then starts. The computation is stopped whenever sensible heat flux at z_r differs from less than 10^{-4} times net radiation between two iterations. In general 3 or 4 iterations are sufficient.

Experimental data set and submodel parameterization

Site description

The experimental site is located at about 20 km from Bordeaux, France (44°43′N, 0°46′W, altitude 62 m) in a homogeneous maritime pine stand (*Pinus pinaster* Ait.) seeded in 1970. The climate is characterized by a strong seasonal contrast in water conditions between winter and spring on the one hand, when rainfall exceeds evaporation, and summer and autumn on the other hand, when water deficit (often accompanied by soil drought) may last for weeks to months. The trees are distributed in parallel rows along a NE–SW axis with an interrow distance of 4 m. In 1997–1998 the stand density was 520 trees ha^{-1}, the mean tree height varied between 17.7 and 18.9 m and the projected leaf area index varied between 2.6 and 3.2. The crowns are on average within the top 6 m (Porté *et al*., 2002) and are therefore well separated from the understorey. The latter mainly consists of grass (*Molinia coerulea*), whose roots and stumps remain throughout the year. The leaves are only present from April to late November, with maximum leaf area index and height of

1.4–2.0 and 0.6–0.8 m, respectively (Loustau & Cochard, 1991). A 5-cm thick litter made of compacted grass and dead needles is present all year long. The water table never goes deeper than about 200 cm. During the (1997–1998) winter its level went up to the soil surface but no runoff was observed, as the terrain is very flat.

Experimental set-up

The experimental set-up that provided the data used here was installed following the requirements of the EUROFLUX network. At 25 m aboveground, considered here as our reference level z_r, the following data was measured every 10 s and averaged every 30 min: net radiation with a *Q*7 net radiometer (REBS, Seattle, USA); incident and upward solar radiation with two C180 pyranometers (Cimel, France); incident and diffuse photosynthetically active radiation; air temperature and specific humidity with a 50Y temperature–humidity probe (Vaisala, Finland). Wind speed, friction velocity and sensible heat flux were measured at the same level with a 3D sonic anemometer (Solent R2, Gill Instruments, Lymington, Hampshire, UK) and water vapour and carbon dioxide fluxes with the sonic anemometer coupled with an infrared gas analyzer (LI-6262, LICOR, Lincoln, Nebraska, USA). Rainfall was measured at 20 m with an ARG100 rain gauge (Young, USA). Incoming long-wave radiation was deduced from net and solar radiation measurements. All other details can be found in Berbigier *et al*. (2001).

Sub-model parameterization

Phenological and structural parameters Crown height and depth, as well as the vertical distribution of the three cohorts of needles, are given by Porté *et al*. (2000). The whole-sided leaf area of each cohort (L_α) is computed with a phenological model developed by Loustau *et al*. (1997) after a study of Desprez-Loustau & Dupuis (1994) on the date of needle emergence (Fig. 1a). In winter the vertical profile of needle area density is expressed for each cohort as a beta function of the relative height within the crown (Porté *et al*., 2000). During the rest of the year the profiles are computed by letting the beta coefficients change linearly throughout the year, while ensuring normalization of the beta function.

Bosc (2000) developed an analytical model to compute the shoot silhouette-to-total area ratio (*STAR*) and the fraction of sunlit needle sections in the shoots (Σ_{sun}). This model makes use of several inputs such as the number of needles on the shoot and their mean insertion angle and diameter. We applied this model to a set of 17 shoots and adjusted simple equations only depending on shoot age (Fig. 1b, c):

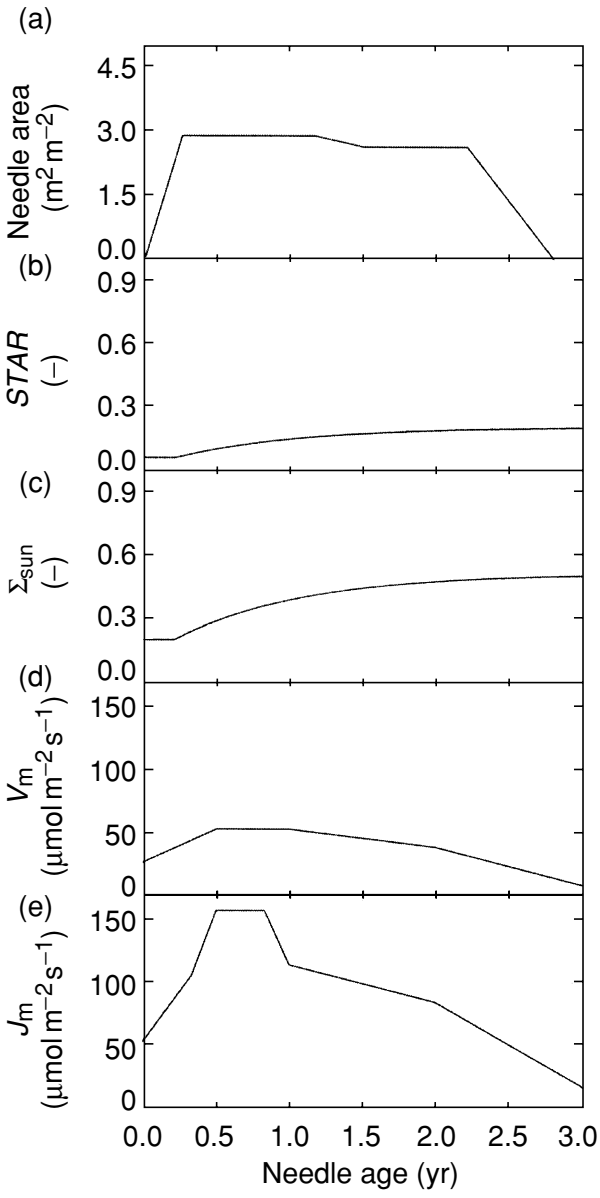

Fig. 1 Modelled age-related variations of whole-sided needle area (a), shoot silhouette-to-total area ratio *STAR* (b), fraction of sunlit needle sections in the shoots Σ_{sun} (c), maximum carboxylation velocity V_m at 25 °C (d) and maximum electron transport rate J_m at 25 °C (e). Needle area variations are taken from Porté (1999), *STAR* and Σ_{sun} variations are modelled after measurements performed by Bosc (1999), V_m and J_m variations are given by Medlyn *et al*. (2002) for needles between 3-months and 1-year-old and by Porté & Loustau (1998) for older needles. For young growing needles, a rapid linear increase is assumed during growth as observed by Wilson *et al*. (2000).

$$STAR_\alpha = 0.06 + (0.21 - 0.06) \times \{1 - \exp[-\max(0\,(Y_\alpha - 0.21)/0.88)]\} \quad (11a)$$

$$\Sigma_{\text{sun},\alpha} = 0.20 + (0.52 - 0.20) \times \{1 - \exp[-\max(0\,(Y_\alpha - 0.21)/0.88)]\} \quad (11b)$$

Regarding now the understorey, the leaf area index is modelled from the measurements of Loustau & Cochard (1991). The leaf angle distribution is allowed to vary along the growing season from a vertical to a nearly spherical distribution. Also the proportion of green leaves in the understorey (γ_u) used in the computation of the understorey albedo is computed in order to equal unity during leaf emergence and full development, then decrease rapidly after the beginning of leaf senescence.

Hydrological parameters Canopy and understorey water storage capacity and throughfall are given by Loustau *et al*. (1992), and the soil and litter structural and hydrological parameters by Ogée & Brunet (2002).

Photosynthetic parameters The photosynthesis model of Farquhar *et al*. (1980) uses four main parameters: the potential electron transport (J_m), the maximum rate of carboxylation (V_m), the quantum efficiency for photosynthesis (α_j) and the dark respiration rate (Rd). For both canopy needles and understorey leaves these parameters are likely to vary temporally during leaf ageing (Wang *et al*., 1995; Porté & Loustau, 1998; Wilson *et al*., 2000) and spatially according to leaf nitrogen content (Wilson *et al*., 2000; Wilson *et al*., 2001). They also depend on leaf temperature with an optimum temperature T_{opt} that may vary seasonally due to leaf acclimation (Law *et al*., 2000; Medlyn *et al*., 2002).

Variations with age were observed at our site for canopy needles (Porté & Loustau, 1998), but spatial variations seem to remain small (Porté & Loustau, 1998) although they have not yet been fully characterized. In addition, Medlyn *et al*. (2002) recently described the seasonal variation in the temperature response of both J_m and V_m for adult maritime pines grown in the same area. They evidenced a significant acclimation in J_m response to the ambient temperature, which was not observed for V_m. We therefore decided to account for the effect of ageing and temperature acclimation on the photosynthetic parameters of the needles. For a given parameter W, variations with needle temperature and needle age or climate are described using:

$$W = W_{\text{ref}} \times f_{\text{leaf temperature}} \times f_{\text{age/climate}} \quad (12)$$

where W_{ref} is the parameter value at 25 °C and for an age or climate of reference and the f's are functions of needle temperature and needle age or climate (Table 2). For V_m and J_m seasonal changes described in Medlyn *et al*. (2002) are supposed to be caused by needle ageing only and are combined with data given by Porté & Loustau (1998) to model the variations of the two parameters along a needle life (Fig. 1d, e). For the optimal J_m temperature the effects of acclimation reported by Medlyn *et al*. (2002) are captured by a function of the maximum air temperature of the previous day (Table 2). The temperature dependency ($f_{\text{leaf temperature}}$) of V_m and J_m for the pine needles is given by Medlyn *et al*. (2002) and that of *Road* is given by Porté & Loustau (1998).

Regarding understorey leaves the reference value and temperature dependency for V_m, J_m and Rd have been characterized experimentally (Delzon *et al*., submitted). No effect of age or climate is accounted for, except during leaf senescence (Table 2).

Stomatal conductance model parameters The parameters used in the stomatal conductance model of Leuning (1995) were determined for shoots from stomatal conductance measurements performed by Bosc (1999) on 7 month-old and 19 month-old shoots over a 40-day period at the end of summer 1997 (days 256–296). For understorey leaves they were determined *in situ* from

Table 2 Reference value and leaf age or climate dependency of model physiological parameters

Parameter and unit	$f_{\text{age/climate}}$
Canopy photosynthesis (Porté & Loustau, 1998; Medlyn *et al*., 2002)	
V_m (μmol m^{-2} s^{-1})	see Fig. 1d
J_m (μmol m^{-2} s^{-1})	see Fig. 1e
α (mol(CO$_2$) mol(photons)$^{-1}$)	0.12
Rd (μmol m^{-2} s^{-1})	0.31
T_{opt} (for J_m) (°C)	$31.8 + 0.16 \times T_{\text{max, m1}}$*
T_{opt} (for V_m) (°C)	38.3
Understorey photosynthesis (Delzon *et al*. submitted)	
J_m (μmol m^{-2} s^{-1})	$35 \times \gamma_u$†
V_m (μmol m^{-2} s^{-1})	$25 \times \gamma_u$
α (mol(CO$_2$) mol(photons)$^{-1}$)	$0.109 \times \gamma_u$
Rd (μmol m^{-2} s^{-1})	$0.17 \times \gamma_u$
T_{opt} (for J_m and V_m) (°C)	36
Canopy stomatal conductance (Bosc, 1999)	
m (–)	12
g_0 (mmol m^{-2} s^{-1})	0
D_0 (hPa)	17
ψ_0 (MPa)	−1.1
v_0 (–)	6
Understorey stomatal conductance (Delzon *et al*. submitted)	
m (–)	10
g_0 (mmol m^{-2} s^{-1})	0
D_0 (hPa)	15
ψ_0 (MPa)	−1.7
v_0 (–)	7

*Daily maximum air temperature of previous day.
†During leaf emergence and full development $\gamma_u = 1$ and no age effect is accounted for.

CO_2 gas-exchange measurements (Delzon *et al.*, submitted). Parameters ψ_0 and v_0 for both canopy and understorey were independently determined from several studies on water stress made at our site (Berbigier *et al.*, 1991; Loustau & Cochard, 1991; Granier & Loustau, 1994). The values are given in Table 2.

Respiration model parameters Bole respiration is parameterized after Bosc *et al.* (2003), using the biomass information of Porté *et al.* (2002). Soil and litter respiration is parameterized from soil respiration measurements performed at our site in 2000–2001 (Loustau *et al.*, 2003), giving $Q_{10} = 2.7$ and a soil CO_2 efflux at 15 °C of $1.68\,\mu mol\,m^{-2}\,s^{-1}$.

Turbulence parameters Turbulent variables were analyzed and modelled by Ogée (2000), using data collected since 1989. During this period the canopy height changed from 13.2 m to 19.5 m. The experimental set-up of each campaign can be found in Brunet & Irvine (2000), Lamaud *et al.* (2001) and Berbigier *et al.* (2001).

Using six months worth of wind speed measurements at two levels above the canopy we adjusted the two parameters used in the roughness sublayer profile of Cellier & Brunet (1992), the sublayer height z^* ($1.37\,h$) and the wind shape factor η (0.47). For comparison Cellier & Brunet (1992) obtained for these two parameters over maize field $1.45\,h$ and $0.45\,h$, respectively. The normalized neutral wind speed at canopy top is 2.9 (Ogée, 2000), which is consistent with the standard value of 3 (Raupach, 1989b). Within the vegetation the horizontal wind speed model of Massman & Weil (1999) was parameterized with a mutual interference coefficient for canopy needles of 2.1 (Grant, 1984; Nikolov *et al.*, 1995). This model allows us to reproduce well the neutral wind speed measurements collected at our site between 1989 and 1999 (Fig. 2a). However it is unable to reproduce correctly the vertical profile of σ_w collected during the same campaigns, probably due to the assumption of the w-variance being proportional to the turbulent kinetic energy in a forest canopy. We therefore adjusted an empirical model, independent of canopy structure (Fig. 2b). At the top of the roughness sublayer we obtain a value of 1.33 ± 0.13 which is consistent with the standard, neutral value of 1.25 (Raupach, 1989b; Leuning *et al.*, 2000). The generic neutral profiles of the Lagrangian time scale T_L and the scalar far-field diffusivity K_f are computed after Massman & Weil (1999), using the σ_w profile described above (Fig. 2c, d).

The stability correction function ϕ_m are parameterized using sonic anemometer measurements at three levels (7, 25 and 43 m) from 1997 to 1999:

$$\phi_m = \begin{cases} (1 - 16z^*/L)^{-0.2} & -2 \le z^*/L \le 0 \\ (1 + 5z^*/L)^{0.4} & 0 \le z^*/L \le 1 \end{cases} \quad (13)$$

The results are illustrated in Fig. 3a. The stability correction function ϕ_w was fitted against the same dataset (Fig. 3b):

$$\phi_w = \begin{cases} (1 - 3z^*/L)^{0.2} & -2 \le z^*/L \le 0 \\ (1 + 0.2z^*/L) & 0 \le z^*/L \le 1 \end{cases} \quad (14)$$

The stability correction function ϕ_h is that used by Leuning (2000), with z^*/L as the atmospheric stability parameter. Equations (13) and (14) are just extensions to the roughness sublayer of the classical formulas used for the surface boundary layer. For this reason, we did not allow the coefficients to vary with height, although this would have provided a better fit.

Model validation

General principles

The model was parameterized as described above, without making any use of the scalar flux measurements

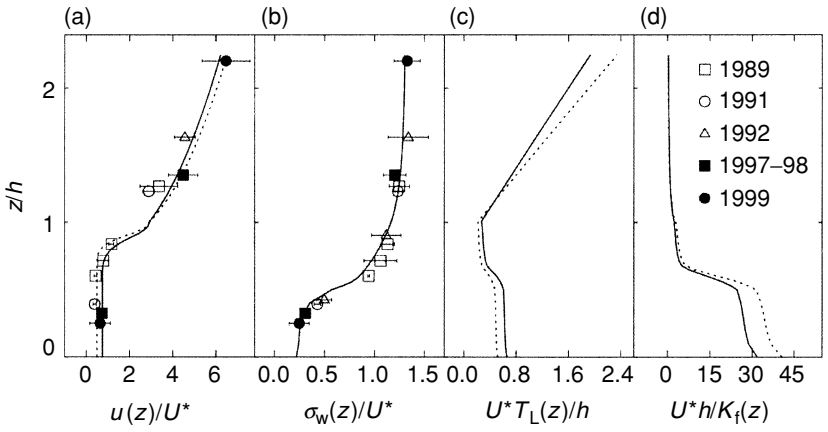

Fig. 2 Normalized profiles of (a) wind speed, (b) standard deviation of vertical velocity, (c) Lagrangian time scale and (d) inverse of far-field diffusivity. Data from different years are indicated with different symbols. Solid and dotted lines indicate the profiles obtained with the model of Massman & Weil (1999) for 1989 and 1999, respectively, except in (b) where we used an empirical model independent of canopy structure (see text).

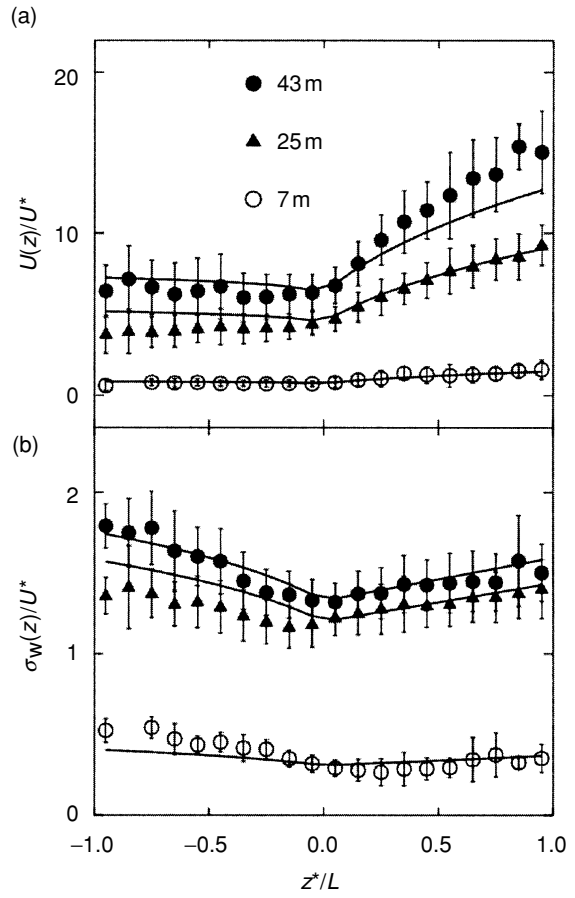

Fig. 3 Stability corrections at different heights (7, 25 and 43-m) for (a) normalized mean wind speed and (b) normalized standard deviation of vertical velocity. Data from different heights are indicated with different symbols and solid lines are the functions given by Eqns (13) and (14).

performed during the EUROFLUX campaign. A direct comparison of the modelled and measured scalar fluxes can therefore be considered as a proper validation test of the model. A grand total of 29 232 half-hourly runs is available for this validation. Occasional missing data for each flux leave 28 876 values for the sensible heat flux, 28 877 for the latent heat flux and 26 525 for the CO_2 flux.

For reasons discussed in the introduction the two-year data set was split up into several seasonal types. It was first felt necessary to distinguish spring–summer days from autumn–winter days. For the sake of simplicity 'summer days' were defined so as to coincide with the period with an active understorey and therefore refer to the period between late spring and early autumn. 'Winter days' refer to the rest of the year. As our site often experiences summer drought, with dramatic consequences on the physiology, we defined two summer classes based on soil water availability. From past experience (Berbigier *et al*., 1991; Granier & Loustau, 1994) a threshold value of 65 mm for bulk soil water content (W_d) is used for this purpose. W_d was measured bi-weekly throughout the experimental period and daily values were interpolated using the following equation (Ogée & Brunet, 2002):

$$\frac{dW_d}{dt} = P_r - E - 0.012 \times (W_d - 80) \qquad (15)$$

where P_r and E are the measured rainfall rate and water vapour flux above the canopy, respectively, and t is time. We therefore have three main seasonal types: winter, well-watered summer and water-stressed summer.

Model testing against instantaneous and accumulated flux data

For each flux four linear regressions between measured and modelled values were performed using the full dataset and the three seasonal subsets. The results are displayed in Table 3. The total root mean square error (RMSE) is decomposed into systematic ($RMSE_s$) and unsystematic ($RMSE_u$) components (Willmott, 1981): large $RMSE_s$ means that the model is biased in a systematic way and leads to large discrepancies between measured and modelled accumulated flux values.

Table 3 shows that *MuSICA* behaves generally well with r^2 values around 0.75 on average. However we notice relatively large intercepts and systematic errors on the latent heat flux in all cases. This result in an increasing difference between the accumulated measured and modelled curves (Fig. 4). The intercepts and the systematic errors are much smaller (less than 7 W m^{-2}) for the sensible heat flux, even if the total RMSE has the same magnitude than in the former case. The discrepancies are therefore mainly non-systematic, which explains the very good agreement in Fig. 4 between accumulated measured and modelled sensible heat fluxes. The CO_2 flux seems to be better captured by *MuSICA* in winter than at any other period. Indeed the slope and intercept in winter are very satisfactory (0.95 and $-0.22\,\mu mol\,m^{-2}\,s^{-1}$, respectively) and the systematic error is small ($0.31\,\mu mol\,m^{-2}\,s^{-1}$). In summer the intercept and the systematic error are large, especially for water-stressed conditions ($1.8\,\mu mol\,m^{-2}\,s^{-1}$ and $2.1\,\mu mol\,m^{-2}\,s^{-1}$, respectively). In fact the model can also give good results in summer: in Fig. 4 the agreement between daily modelled and measured CO_2 fluxes is good during the full period except in summer 1997, and the two accumulated CO_2 flux curves are in good agreement until day 200 where they steadily diverge until day 300; then they remain separated by a nearly equal distance until the end of the two-year period.

The statistics presented in Table 3 and the accumulated fluxes plotted in Fig. 4 are useful to get a general feeling on the model behaviour. However, once the fluxes and

seasons for which the model systematically diverges from the measurements have been identified, it is necessary to further analyze the reasons for these discrepancies. For example we conclude from Fig. 4 that *MuSICA* underestimates the CO_2 sink strength during summer 1997 but seems to behave well during summer 1998. Yet, both years are marked by low soil water levels. To better understand this interannual variability it appears sensible to characterize days not only in terms of seasons and soil water availability but also in terms of weather types.

Model behaviour according to seasonal and weather types

For each seasonal type described above we set a threshold value of 40% for diffuse radiation in order to separate cloudy and overcast days from clear days and days with passing clouds, and a threshold value of 5 hPa on mean daily vapour pressure deficit (VPD) in order to separate moist air conditions from dry air conditions. This procedure leads to four weather types (sunny-moist, sunny-dry, cloudy-moist and cloudy-dry). Combined with the three seasonal types, we end up with 12-day types. The distribution of these types throughout the two-year experimental period is shown in Fig. 5. The number of days per type is generally larger than 30 (Fig. 6). The most common types (more than 100 days each) are 'cloudy moist winter', 'well-watered sunny dry summer' and 'well-watered cloudy moist summer'. Three types are poorly represented ('cloudy dry winter', 'water-stressed sunny moist summer' and 'water-stressed cloudy dry summer'), but they were kept for the analysis because they represent 'extreme' weather conditions.

Measured and modelled 30-min fluxes are displayed in Fig. 6 for each day type. It can be seen that the model reproduces reasonably well the daily variations in the three fluxes for most weather types. However systematic discrepancies are visible, that can be listed as follows.

1. Under sunny dry conditions during winter the model predicts higher rates of transpiration and photosynthesis, although this only contributes to a small extent to the divergence between modelled and measured accumulated fluxes, as is visible in Fig. 4. This behaviour may be due to an inadequate description of the stomatal response of the needles to VPD and low air temperature. Indeed, at this time of the year, only canopy needles are active and their stomatal response to VPD has been parameterized from gas exchange measurements performed in summer. A unique set of parameters has therefore been used but several studies have evidenced variations in the response to VPD with the season (Whitehead *et al*., 1984; Medlyn *et al*., 2002).
2. In dry summer conditions CO_2 assimilation is underestimated (at least in well-watered summer). This explains why the modelled accumulated CO_2 flux curve in Fig. 4 goes over the measured curve in summer 1997 (around day 170) and then increases up to day 259 (excluding days 231–239, that belong to 'water-stressed summer'). The divergence between the two curves is mainly visible in 1997, partly because

Table 3 Statistical results of the linear regression between half-hourly measured and modelled fluxes

	Slope	Intercept	r^2	RMSE	$RMSE_u$	$RMSE_s$	n
Latent heat flux ($W m^{-2}$)							
All	0.86	17	0.76	43	41	15	28 877
Winter	0.91	11	0.70	35	34	9.5	10 434
Well-watered summer	0.84	22	0.77	50	47	19	13 344
Water-stressed summer	0.82	18	0.70	39	35	16	5 099
Sensible heat flux ($W m^{-2}$)							
All	0.97	1.7	0.78	44	44	2.4	28 876
Winter	0.91	− 0.40	0.76	40	40	6.7	10 434
Well-watered summer	0.99	4.2	0.76	47	47	4.0	13 343
Water-stressed summer	1.01	−2.3	0.85	42	42	2.1	5 099
CO_2 flux ($\mu mol\, m^2\, s^{-1}$)							
All	0.83	0.39	0.70	3.8	3.6	1.3	26 525
Winter	0.95	−0.22	0.78	2.6	2.6	0.31	10 004
Well-watered summer	0.79	0.39	0.72	4.4	3.9	1.9	12 103
Water-stressed summer	0.83	1.8	0.53	4.4	3.9	2.1	4 418

Slopes and intercepts are computed using an orthogonal regression (Press *et al*., 1992), r^2 is the linear correlation coefficient, RMSE is the root mean square error that is decomposed into unsystematic ($RMSE_u$) and systematic ($RMSE_s$) components and n is the number of data points.

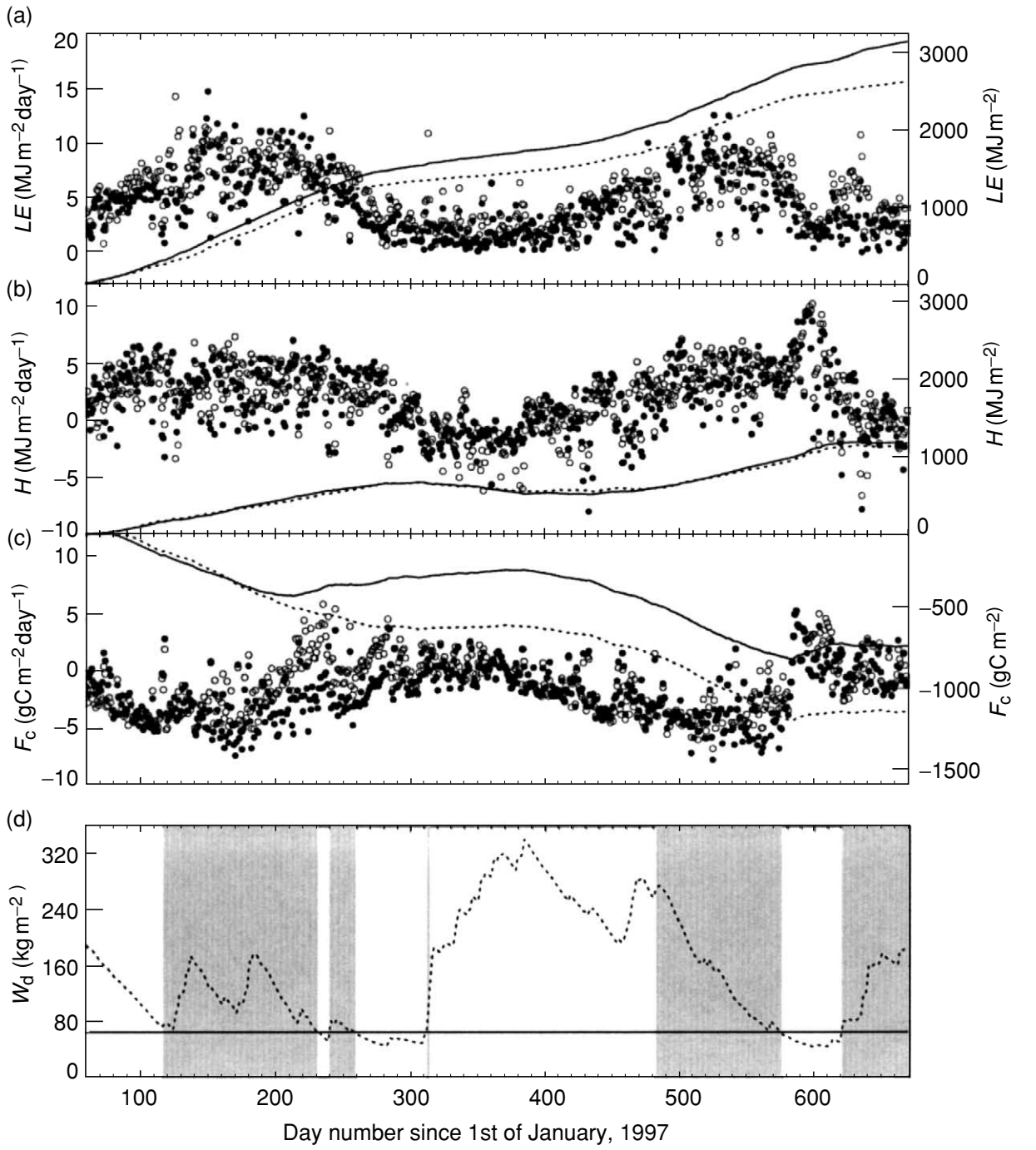

Fig. 4 Daily and cumulative fluxes of latent heat (a), sensible heat (b) and CO_2 (c) at 'Le Bray' from March 1997 to October 1998. Both measured (closed circles and dotted line) and modelled (open circles and solid line) values are shown. In (d) soil water content is displayed, as computed from Eqn (15) (dotted line), along with the threshold value used to distinguish well watered from water-stressed periods in summer (solid line). Well-watered summer periods are indicated in grey.

summer 1997 has a larger proportion of days with very dry air than summer 1998 (see Fig. 5). However, 1997 is also characterized by much lower levels of soil water, as compared with 1998: in summer 1997 soil water content always remains at low levels, especially at the beginning (around day 117, when young needles are emerging), in the middle (around day 170) and at the end (from day 225). In contrast, in 1998, W_d takes low values only at the end of summer. For this reason we think that the stomatal response

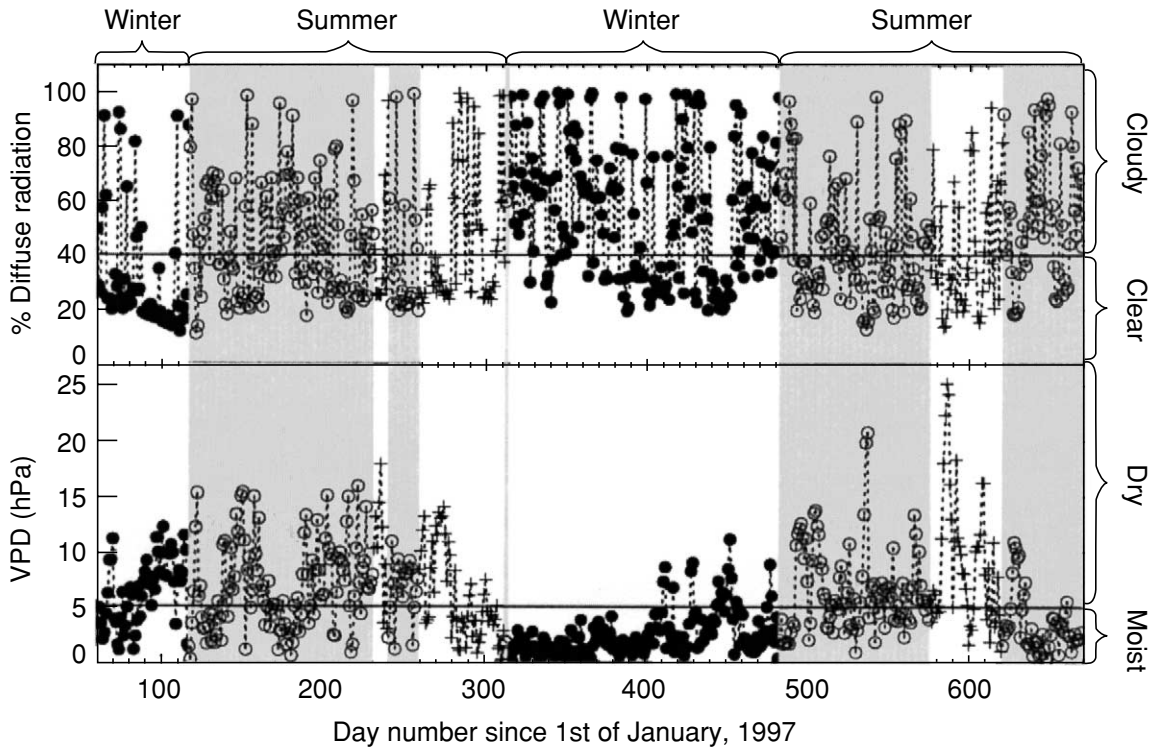

Fig. 5 Daily mean fraction of diffuse radiation (a) and daily mean water vapour deficit (b) measured at 'Le Bray' from March 1997 to October 1998. Winter days (●), well watered summer days (○) and water-stressed summer days (+) have been distinguished. Horizontal solid lines indicate the threshold values used to classify days by weather type for each seasonal type. Well-watered summer periods are indicated in grey.

to VPD should not be incriminated here, but rather the stomatal response to soil water content, or a possible interaction between soil water content and stomatal response to VPD or photosynthesis. Indeed the disagreement between model and measurements in Fig. 4 starts around day 145, whereas high levels of VPD also occur at the beginning of summer 1997 (Fig. 5). This suggests that, over the period between days 117 and 145, the stomatal response of needles or leaves to high VPD levels is well accounted for in *MuSICA*, despite the low to intermediate values taken by W_d. From day 145 onwards VPD values are not particularly larger but W_d decreases again just above the threshold value of 65 mm. Obviously the modelled stomatal conductance in *MuSICA* is too strongly reduced at this time of the year, when W_d takes intermediate values. This reduction in stomatal conductance mainly affects the CO_2 flux, as leaf transpiration is little sensitive to g_s at such high VPD levels. As noted above the functions used to relate the stomatal conductance and soil water availability are empirical. They are valid at the lowest range of W_d but need some refinement at intermediate levels.

3. In dry water-stressed summer conditions soil respiration is clearly overestimated. This effect adds up with that described above and is responsible to a large extent for the disagreement in Fig. 4 between modelled and measured CO_2 fluxes. The effect of water stress on soil respiration, which is not accounted for in our model, should be incriminated here. The data used to fit our soil/litter respiration model covered periods with low soil water levels. Yet, at the present stage, it has not seemed possible to elaborate a proper, robust soil/litter respiration model that could accommodate for water stress effects for our site and data basis. Figure 6 clearly shows that soil respiration is not reduced during all summer water-stressed days but only when the air is dry, which occurs when it has not rained for some time (sunny and cloudy dry periods together represent only 1.6 mm of water, for a total of 61 days in the present data set). This suggests that soil respiration reacts to litter or soil surface moisture rather than bulk soil water. However soil respiration includes various processes such as root growth, microbial activity and CO_2 dissolution in soil water that have presumably different response times to soil water stress and soil rewetting.

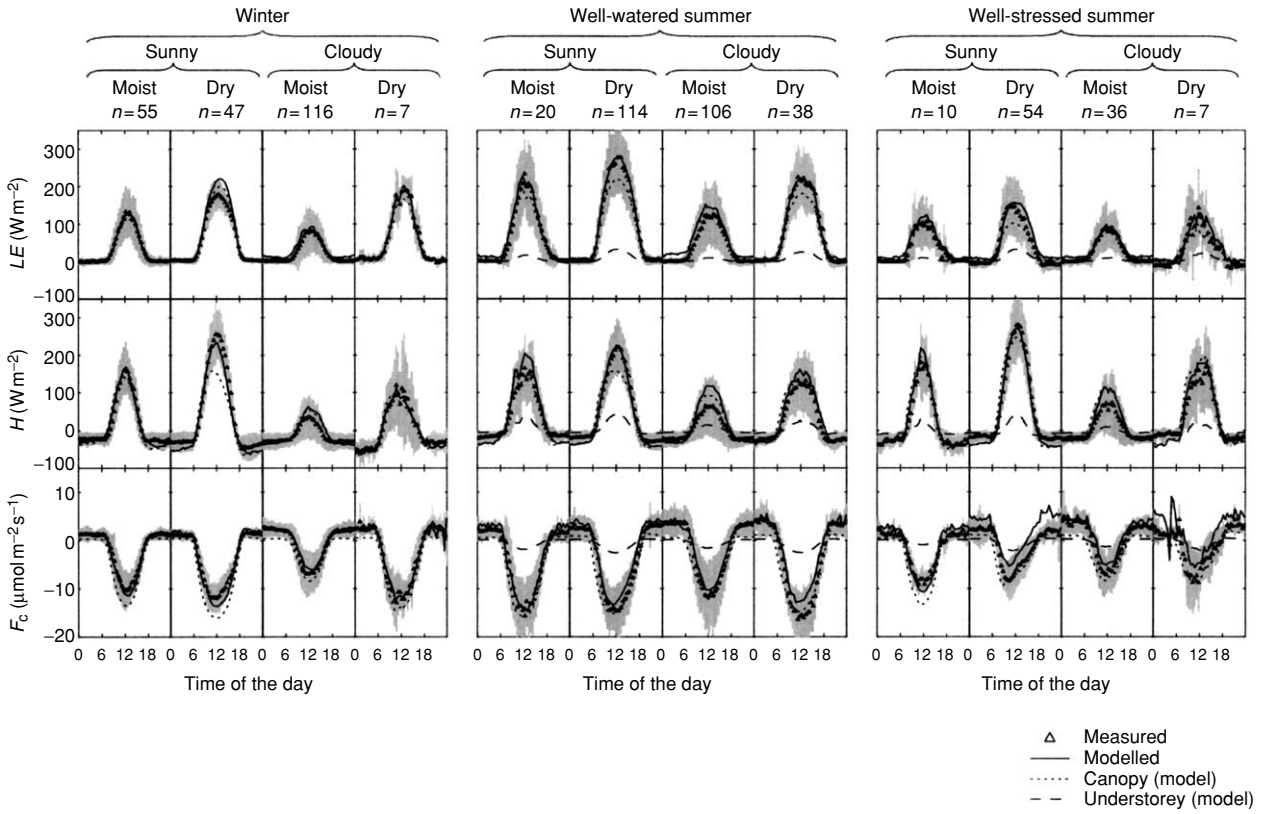

Fig. 6 Mean turbulent fluxes above the canopy of latent heat (*LE*), sensible heat (*H*) and CO_2 (F_c) at 'Le Bray' from March 1997 to October 1998 and for the 12 different weather and seasonal types. Both measured (open triangles) and modelled (solid line) values are shown. For modelled values the relative contribution of canopy (dotted line) and understorey (dashed line) are also displayed. For measured values the standard deviation is indicated in grey.

4. For all seasons in cloudy moist conditions, the model gives larger latent and sensible heat flux values. As this weather type is most common at our site (116 days and 106 days over the 1997–1998 period in winter and well-watered summer, respectively), the differences between measured and modelled accumulated values of latent heat flux are relatively large. Regarding the sensible heat flux, the good agreement in Fig. 4 results to some extent from compensation between this effect and a slight but constant underestimation during the night. It must be pointed out that these periods are often affected by rain. Indeed, in cloudy moist conditions, the percentage of time with rain is 18, 16 and 11% in winter, well-watered and water-stressed summer, respectively, whereas it averages around only 2% for all other weather types. During rain events the eddy-covariance method is prone to large errors and gap-filling algorithms are used to produce continuous flux data files (Berbigier *et al*., 2001; Falge *et al*., 2001a, b; Wilson *et al*., 2002). In fact gap-filled *H*-values correspond to identified sonic anemometer breakdown periods (Berbigier *et al*., 2001), which do not always correspond to rain events. Therefore during these events measured *H*-values, if not corrected, may be underestimated, as raindrops on the anemometer tend to attenuate the signal. The *LE* values corresponding to rain events may also be underestimated. This even affects gap-filled values because the resistance to evaporation is always smaller than the resistance to transpiration and gap-filling algorithms are estimated from data collected when the vegetation is only transpiring. This may explain why *MuSICA* predicts higher rates of latent and sensible heat than measured or gap-filled values. High rates of sensible heat flux in the model may also be due to the fact that two separate energy budgets for wet and dry leaves are performed in *MuSICA*. Watanabe & Mizutani (1996) developed a multilayer rain interception model with only one leaf temperature and one energy budget in each layer. Their model correctly simulates a nearly zero sensible heat flux for one light rain event that occurred during the day. In contrast *MuSICA* predicts negligible sensible heat fluxes only during heavy rain events (> 10 mm per day), in accordance

with the measurements. However during light rain events the model overestimates almost systematically the sensible heat flux. The approach of Watanabe & Mizutani (1996) may better perform in this case. Only a direct comparison of the two modelling strategies could help answer this question.

Model simplification and sensitivity analysis

All the results previously shown were obtained with the 'full version' of *MuSICA* in which sunlit, shaded, wet and dry leaves, and 0, 1 and 2 years-old needles are distinguished. A total of 12 layers are used between the ground and the reference level, with 10 layers in the forest, amongst which four are located in the crown space. As mentioned in the introduction, it is highly desirable to investigate the usefulness of distinguishing so many 'big leaves' and layers. In this section we test a series of simplifications. All results are presented in terms of root mean square errors (RMSE) on 30-min turbulent fluxes normalized with RMSE values given by the reference simulation. A RMSE ratio larger than 1 means that the model performance is reduced compared to the reference version (in the sense of RMSE). The results are given for the full dataset and for each of the 12-day types (Fig. 7).

Few studies have addressed such issues. The influence of distinguishing sunlit and shaded leaves has been studied by de Pury & Farquhar (1997). They concluded that the division of leaf area into sunlit and shaded portions is essential as compared to using averaged radiation. As a first sensitivity test we ran a version of *MuSICA* where all needle segments at a given level z_j are subject to one light regime, equal to $Q_{abs,b,\alpha,j}/\Sigma_{sun,\alpha} \times P_{sun,\alpha,j} + Q_{abs,d,\alpha,j}$. The results, shown in Fig. 7a, confirm those found by de Pury & Farquhar (1997), especially under clear sky conditions where RMSE ratios are much larger than 1 for all fluxes.

A second sensitivity test consists in considering only dry leaves or needles. For this we assume that vegetation does not intercept rain, i.e., its water storage capacity is zero. The summation in Eqn (9) is then performed over dry needles only ($P_{wet,\alpha,j} = 0$). Figure 7b shows that the

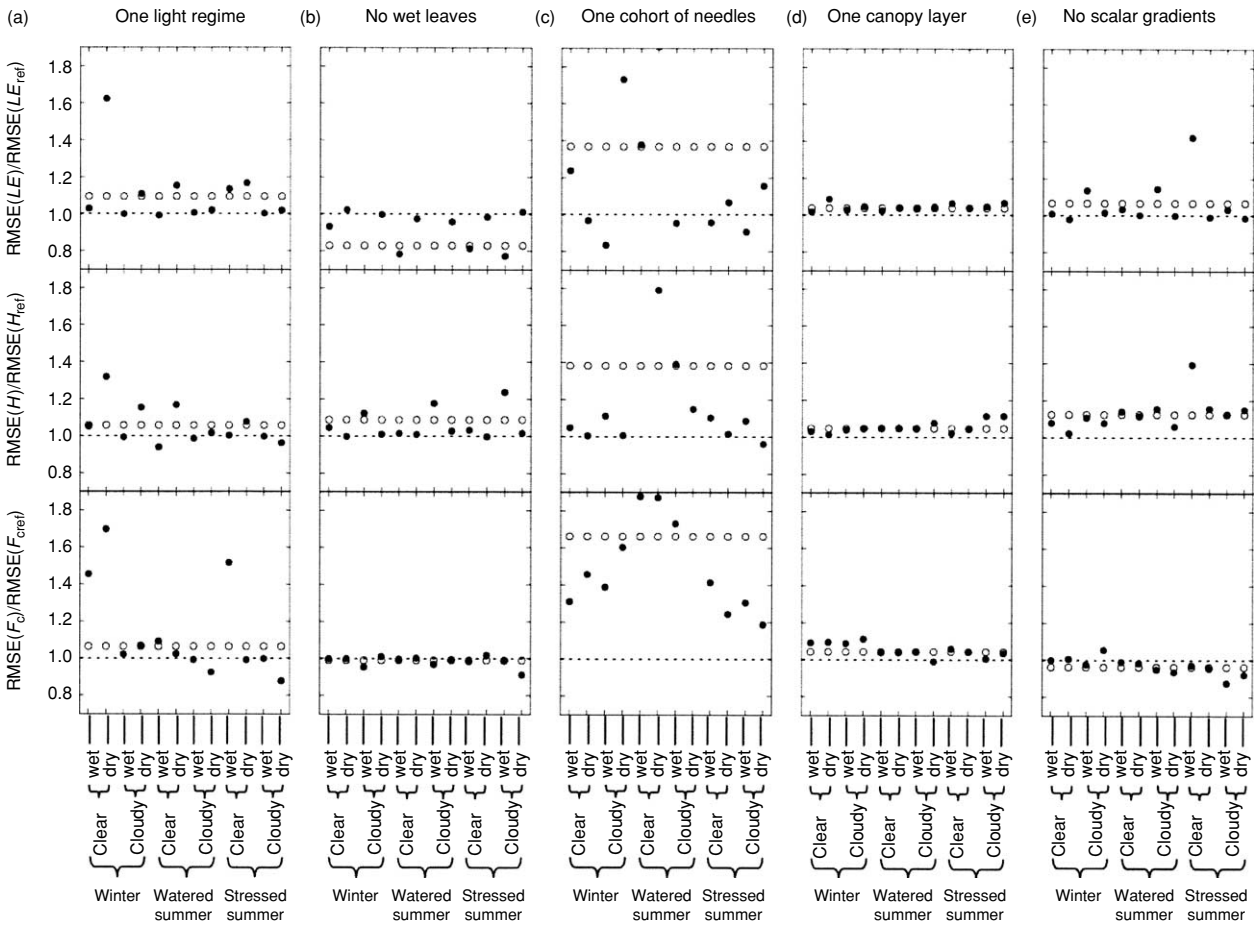

Fig. 7 Root mean square errors (RMSE) between modelled and measured 30-min fluxes using either the full dataset (○) or each subset corresponding to a day type (●), for five different versions of *MuSICA* (see text). The results are normalized by the RMSE given by the reference version of the model so that a RMSE ratio of 1 means that there is no degradation, as compared to the reference version.

average CO_2 flux is little affected, regardless of the weather type. This demonstrates that the CO_2 flux from wet leaves is a minor component of the total ecosystem carbon exchange. Sensible and latent heat fluxes are affected, but mostly under cloudy/moist conditions as they include most of the rain events. The total root mean square error ratios are then greater than 1 for *H* and smaller than 1 for *LE*, because both fluxes are linked by the energy budget. The main effect of ignoring water storage by vegetation is to increase leaf/needle surface temperature during rain events, which leads to higher values of *H* and smaller values of *LE*. The increase in sensible heat flux leads to greater RMSE for *H* and smaller RMSE for *LE* because the sensible and latent heat fluxes simulated with the 'full version' of *MuSICA* were already too high as compared to the measurements (see Fig. 4). However no further analysis should be made, because of the questionable quality of both the modelling strategy used in *MuSICA* to compute the surface temperature of wet leaves and the experimental data for this type of weather (see previous section).

Considering only one age class in the canopy layers is relevant here because a specificity of *MuSICA* is to account for the differences in age classes. For this we suppressed the distinction between 0, 1 and 2 years-old needles, i.e., we considered only four 'big shoots' in each canopy layer (sunlit/dry, shaded/dry, sunlit/wet and shaded/wet). All shoots are then supposed to have the same *STAR* and Σ_{sun} and the same photosynthetic and respiratory parameters (J_m, V_m, α_j and *Road*) computed as an average over all age classes with weighting factors L_α. The results are shown in Fig. 7c. It can be seen that this simplification severely reduces the model performance, with an increase in RMSE values of about 40–70%. This is particularly true in well-watered summer because the shape and photosynthetic capacity of the young shoots are quite different from those of the older shoots. Using an average value for *STAR*, Σ_{sun}, V_m and J_m leads to an overestimation of the radiation absorbed by young shoots and an increase in the CO_2 assimilation of older shoots. Wilson *et al*. (2001) showed that the seasonal variation in the photosynthetic parameters in a mixed deciduous forest is required to estimate accurately the annual net ecosystem exchange. We extend this result here to a coniferous species that has a larger needle longevity (about three years).

Following de Pury & Farquhar (1997) we also tested the influence of the number of canopy layers. We ran a version of *MuSICA* with only one layer in the crown space instead of four layers in the 'full version'. In order to respect the vegetation geometry, a sufficient number of layers have to remain in the nearly 12-m-high spaces between the understorey and the canopy (Wu *et al*., 2000). The total number of layers is then reduced to six layers with five layers within the vegetation. The results in Fig. 7d show that the model turns out to be almost insensitive to the number of canopy layers. This may suggest that the number of layers in the 'full version' is essentially not enough. According to Norman (1979) the number of canopy layers should be chosen so that leaf area is less than $0.5\,m^2\,m^{-2}$ in each layer. Indeed, when using Beer's law for light attenuation (see Eqn (3)), we implicitly assume that the probability of leaf overlap in a layer is small. In our case the canopy leaf area index is around 3 so that Norman's criteria is violated. However radiative measurements performed at this site showed that Eqn (3) is valid (Berbigier & Bonnefond, 1995; Hassika *et al*., 1997). In addition coniferous leaves (needles) overlap mainly within shoots, which is accounted for in *MuSICA* through the concept of silhouette-to-total area ratio. We think that the insensitivity to the number of canopy layers in the computation of energy and scalar fluxes is explained by the fact that the heterogeneity within the canopy is preserved because several 'big shoots' are distinguished within each layer. This result is in accordance with de Pury & Farquhar (1997).

Our last sensitivity test consists in checking the utility of accounting for scalar gradients within the canopy air space (Eqn (7)). For this, we assume that the scalar variables at all levels are equal to their value at z_r, while the computation of wind speed, friction velocity and the stability parameter is still performed. We can see in Fig. 7e that turbulent transfer is rather important for sensible and latent heat flux but does not seem to affect the computation of the CO_2 flux. At short time scale this effect is particularly visible at night, when the atmosphere is stratified. If turbulent transfer is not accounted for in the model the nighttime sensible heat flux is underestimated (it takes large negative values), which tends to increase the latent heat flux. On a yearly basis, *H* is the most sensitive flux as it is reduced by nearly 14% when turbulent transfer is not accounted for in *MuSICA*, whereas *LE* increases by only 2.5%. Baldocchi & Wilson (2001) performed similar sensitivity tests with the multilayer biophysical model CANOAK and found the same tendency.

Conclusion

In this paper we presented a multilayer, multileaf process-based biosphere–atmosphere gas exchange model (*MuSICA*). This model is particularly designed for coniferous species because it can deal with needle clumping and various age classes of shoots. In order to evaluate the model performance, we used a nearly two-year dataset of continuous water vapour, sensible heat and CO_2 flux measurements collected in a maritime pine forest near Bordeaux (France). Each submodel was parameterized

independently, using the outcomes of several eco-physiological and micrometeorological studies conducted at this site. Special care was taken to capture all the seasonal or acclimation changes of the different parameters.

Generally speaking, the model was able to capture reasonably well the mean 30-min variations in all three turbulent fluxes. However a systematic bias between measured and modelled fluxes was noticeable for latent heat in all seasons and for CO_2 in summer (Table 3 and Fig. 4). In comparison the sensible heat flux is unbiased and accumulated values agree very well.

Grouping days in terms of seasonal types (winter, well-watered summer and water-stressed summer) and weather conditions (sunny-moist, sunny-dry, cloudy-moist, cloudy-dry), and examining the mean fluxes for each day type allowed us to analyze the model behaviour in more details, while keeping most of the information contained in all time scales. Comparing simulated and measured fluxes in relation to seasonal types and weather conditions lead to four identified conditions in which the model disagreed with measurements.

1. In winter we noticed a disagreement between modelled and measured CO_2 and latent heat fluxes for sunny conditions, which represented about 5–10% of the yearly-accumulated fluxes. This effect was attributed to an overestimation of the stomatal conductance of needles. A more mechanistic stomatal conductance model that could accommodate for the seasonal variations in the stomatal response to VPD or its sensitivity to low temperature should improve the model behaviour in winter (Medlyn *et al.*, 2002).
2. In dry summer, and particularly in 1997, CO_2 assimilation was underestimated by the model. In contrast during summer 1998 the model matched the accumulated CO_2 flux variations very well. Contrarily to summer 1998, soil water content in 1997 remained just above the threshold value used to define soil water-stressed conditions. This year-to-year variability was therefore attributed to an inadequate representation of the stomatal response to soil water content, or a possible interaction between soil water content and stomatal response to VPD or photosynthesis. A better and more mechanistic description of the hydraulic system within the plants should improve the model behaviour in summer with intermediate to low soil water levels.
3. In water-stressed summer we noticed a strong overestimation of the soil (or ecosystem) respiration, especially during dry periods which are unaffected by rain. This suggests that respiration is subject to a high day-to-day variability during drought periods and soil re-wetting and that it responds mostly to litter or soil surface moisture. However, at the present stage, it did not seem possible to elaborate a proper, robust soil/litter respiration model that would account for such variability.
4. For all seasons in cloudy-moist conditions we noticed a disagreement between modelled and measured energy fluxes. Such conditions mainly occur during rainy events, when the eddy-covariance method is affected by large errors. Also, because of the questionable quality of both the modelling strategy used in *MuSICA* to compute surface temperature of wetted leaves and the experimental data for this type of weather, it was not possible to elucidate which value, between model and measurements, was the most reliable. Watanabe & Mizutani (1996) suggested a different approach to compute surface temperature of wetted leaves that should be tested in the future.

It is worth pointing out that an analysis relying on cumulative flux values only would not have made such investigation possible, or would have led to erroneous conclusions on the model parameterization. In fact our study suggests that the photosynthetic and structural parameters are correctly described by the model, which represent reasonably well their seasonal variation. This is not so for the stomatal response to VPD or the soil/litter respiration model, which seem subject to variations not accounted for by the model.

As a sensitivity test we also derived and evaluated simpler versions of *MuSICA* (with less layers or without the distinction between sunlit and shaded or wet and dry leaves, ...). Few studies have been conducted on this topic, which is nonetheless essential for a good modelling strategy. One important point is that turbulent transport within the vegetation appears to be crucial to get scalar gradients and sensible or latent heat fluxes, whereas it seems to play a minor role on accumulated CO_2 flux estimates. Similar findings were obtained by Baldocchi & Wilson (2001). de Pury & Farquhar (1997) state that the distinction between sunlit and shaded leaves is of prior importance for computing surface fluxes, and that multi-layer models are not superior to a one layer sun/shade model. We confirm here their finding and extend it to coniferous species with several age classes of needles. We found that a single canopy layer (amongst a total of five vegetation layers) appears to be sufficient to get accurate flux estimates, provided several leaf classes are distinguished. In contrast quite erroneous flux estimates are obtained when the distinction between sunlit and shaded leaves or needles and between the different age classes of needles is omitted. These results indicate that in the context of global-scale modelling studies, where SVAT models are coupled with Global Circulation Models, it might be more sensible to design simple one-layer surface models with sufficient information on leaf

distribution than multilayer models with just one 'big leaf' in each layer. The question remains widely open and should be addressed in the near future.

Finally our results emphasize the fact that SVAT models should always be validated on more than one flux. Indeed dealing with only one flux (e.g. the CO_2 flux) can lead to erroneous conclusions regarding the model. This should be feasible in the Fluxnet network, where continuous measurements of several turbulent fluxes (at least the three we used here) are performed at each site.

Acknowledgements

The authors would like to thank Drs A. Granier, E. Dreyer and R. Dewar for helpful discussions. We also thank two anonymous reviewers for their critical comments on an earlier version of the manuscript. This work was performed during the EUROFLUX project supported by the European Commission under contract ENV4-CT95-0078 (Environment and Climate Programme).

References

Aubinet M, Grelle A, Ibrom A *et al.* (2000) Estimates of the annual net carbon and water exchange of forests: the EUROFLUX methodology. *Advances in Ecological Research*, **30**, 113–175.

Baldocchi DD, Falge E, Gu L *et al.* (2001b) FLUXNET: a new tool to study the temporal and spatial variability of ecosystem-scale carbon dioxide, water vapor, and energy flux densities. *Bulletin of American Meteorological Society*, **82** (11), 2415–2434.

Baldocchi D, Falge E, Wilson K (2001a) A spectral analysis of biosphere–atmosphere trace gas flux densities and meteorological variables across hour to multi-year time scales. *Agricultural and Forest Meteorology*, **107**, 1–27.

Baldocchi DD, Harley PC (1995) Scaling carbon dioxide and water vapour exchange from leaf to canopy in a deciduous forest. II. Model testing and application. *Plant, Cell and Environment*, **18**, 1157–1173.

Baldocchi DD, Wilson KB (2001) Modelling CO_2 and water vapour exchange of a temperate broadleaved forest across hourly to decadal time scales. *Ecological Modelling*, **142**, 155–184.

Baldocchi DD, Wilson KB, Gu L (2002) How the environment, canopy structure and canopy physiological functioning influence carbon, water and energy fluxes of a temperate boradleaved deciduous forest – an assessment with the biophysical model CANOAK. *Tree Physiology*, **22**, 1065–1077.

Berbigier P, Bonnefond J-M (1995) Measurement and modelling of radiation transmission within a stand of maritime pine (*Pinus pinaster* Aït.). *Annales Des Sciences Forestières*, **52**, 23–42.

Berbigier P, Bonnefond J-M, Mellmann P (2001) CO_2 and water vapour fluxes for 2 years above Euroflux forest site. *Agricultural and Forest Meteorology*, **108**, 183–197.

Berbigier P, Diawara A, Loustau D (1991) Etude microclimatique de l'effet de la sécheresse sur l'évaporation d'une plantation de pins maritimes et du sous-bois. *Annales Des Sciences Forestières*, **22**, 157–177.

Bosc A (1999) *Etude expérimentale du fonctionnement hydrique et carboné des organes aériens du pin maritime* (*Pinus pinaster* Aït.) PhD Thesis, Université Victor Segalen – Bordeaux II, Bordeaux.

Bosc A (2000) EMILION, a tree functional-structural model: presentation and first application to the analysis of branch carbon balance. *Annals of Forest Science*, **57**, 555–569.

Bosc A, Loustau D, de Grancourt A (2003) Variability of stem and branch maintenance respiration in a *Pinus pinaster* tree. *Tree Physiology*, **23**, 227–236.

Bouten W, Schaap MG, Aerts J *et al.* (1996) Monitoring and modelling canopy water storage amounts in support of atmospheric deposition studies. *Journal of Hydrology*, **181**, 305–321.

Bristow KL, Campbell GS, Papendick RI *et al.* (1986) Simulation of heat and moisture transfer through a surface residue-soil system. *Agricultural and Forest Meteorology*, **36**, 193–214.

Brunet Y, Irvine MR (2000) The control of coherent eddies in vegetation canopies: streamwise structure spacing, canopy shear scale and atmospheric stability. *Boundary-Layer Meteorology*, **94**, 139–163.

Canadell JG, Mooney HA, Baldocchi DD *et al.* (2000) Carbon metabolism of the terrestrial biosphere: a multi-technique approach for improved understanding. *Ecosystems*, **3**, 115–130.

Cellier P, Brunet Y (1992) Flux-gradient relationships above tall plant canopies. *Agricultural and Forest Meteorology*, **58**, 93–117.

Cescatti A (1998) Effects of needle clumping in shoots and crowns on the radiative regime of a Norway spruce canopy. *Annales Des Sciences Forestières*, **55**, 89–102.

Chen JM, Black TA (1992) Defining leaf area index for non-flat leaves. *Plant, Cell and Environment*, **15**, 421–429.

Delzon S, Medlyn BE, Loustau D (in press) Estimate of understorey contribution to the carbon assessment of a maritime pine ecosystem (*Pinus pinaster* Ait.) in the Southwest of France. *Annals of Forest Science.*

Desprez-Loustau M-L, Dupuis F (1994) Variation in the phenology of shoot elongation between geographic provenances of maritime pine (*Pinus pinaster*) – implications for the synchrony with the phenology of the twisting rust fungus, *Melampsora pinitorqua*. *Annales Des Sciences Forestières*, **51**, 553–568.

Falge E, Baldocchi D, Olson R *et al.* (2001a) Gap filling strategies for defensible annual sums of net ecosystem exchange. *Agricultural and Forest Meteorology*, **107**, 43–69.

Falge E, Baldocchi D, Olson R *et al.* (2001b) Gap filling strategies for long term energy flux data sets. *Agricultural and Forest Meteorology*, **107**, 71–77.

Farquhar GD, von Caemmerer S, Berry JA (1980) A biochemical model of photosynhetic CO_2 assimilation in leaves of C3 species. *Planta*, **149**, 78–90.

Granier A, Loustau D (1994) Measuring and modelling the transpiration of a maritime pine canopy from sap-flow data. *Agricultural and Forest Meteorology*, **71**, 61–81.

Grant RH (1984) The mutual interference of spruce canopy structural elements. *Agricultural and Forest Meteorology*, **32**, 145–156.

Gu L, Shugart HH, Fuentes JD *et al.* (1999) Micrometeorology, biophysical exchanges and NEE decomposition in a two-story boreal forest – development and test of an integrated model. *Agricultural and Forest Meteorology*, **94**, 123–148.

Hassika P, Berbigier P, Bonnefond J-M (1997) Measurement and modelling of the photosynthetically active radiation transmitted in a canopy of maritime pine. *Annales Des Sciences Forestières*, **54**, 715–730.

Jacobs AFG, van Boxel JH, Shaw RH (1992) The dependance of canopy layer turbulence on within-canopy thermal stratification. *Agricultural and Forest Meteorology*, **58**, 247–256.

Katul G, Lai C-T, Shäfer K *et al.* (2001) Multiscale analysis of vegetation surface fluxes: from seconds to years. *Advances in Water Resources*, **24**, 1119–1132.

Lamaud E, Ogée J, Brunet Y *et al.* (2001) Validation of eddy flux measurements above the understorey of a pine forest. *Agricultural and Forest Meteorology*, **106**, 187–203.

Landsberg JJ, Powell DBB (1973) Surface exchange characteristics of leaves subject to mutual interference. *Agricultural Meteorology*, **12**, 169–184.

Law BE, Williams M, Anthoni PM *et al.* (2000) Measuring and modelling seasonal variation of carbon dioxide and water vapour exchange of a *Pinus ponderosa* forest subject to soil water deficit. *Global Change Biology*, **6**, 613–630.

Leclerc MY, Beissner KC (1990) The influence of atmospheric stability on the budgets of the Reynolds stress and turbulence kinetic energy within and above a deciduous forest. *Journal of Applied Meteorology*, **29**, 916–933.

Leuning R (1995) A critical appraisal of a combined stomatal-photosynthesis model for C_3 plants. *Plant, Cell and Environment*, **18**, 339–355.

Leuning R (2000) Estimation of source/sink distribution in plant canopies using Lagrangian dispersion analysis: corrections for atmospheric stability and comparison with a multilayer canopy model. *Boundary-Layer Meteorology*, **96**, 293–314.

Leuning R, Denmead OT, Miyata A *et al.* (2000) Source/sink distributions of heat, water vapour, carbon dioxide and methane in a rice canopy estimated using Lagrangian dispersion analysis. *Agricultural and Forest Meteorology*, **104**, 233–249.

Leuning R, Kelliher FM, de Pury DGG *et al.* (1995) Leaf nitrogen, photosynthesis, conductance and transpiration: scaling from leaves to canopies. *Plant, Cell and Environment*, **18**, 1183–1200.

Loustau D, Berbigier P, Granier A (1992) Interception loss, throughfall and stemflow in a maritime pine stand. 2. An application of Gash's analytical model of interception. *Journal of Hydrology*, **138**, 469–485.

Loustau D, Berbigier P, Kramer K (1997) Sensitivity of the water balance of south-western-France maritime pine forests to climate. In: *Impacts of Global Change on Tree Physiology and Forest* (eds Mohren GMJ, Kramer K, Sabaté S), pp. 193–207. Kluwer Academic Publishers, The Netherlands.

Loustau D, Cochard H (1991) Utilisation d'une chambre de transpiration portable pour l'estimation de l'évapotranspiration d'un sous-bois de pin maritime à molinie (*Molinia coerulea* (L) Moench). *Annales Des Sciences Forestières*, **48**, 29–45.

Loustau D, Delzon S, Bosc A *et al.* (in press) Soil CO_2 efflux in a chronosequence of maritime Pine stands. *Annals of Forest Science.*

Massman WJ, Weil JC (1999) An analytical one-dimensional second-order closure model of turbulence statistics and the Lagrangian time scale within and above plant canopies of arbitrary structure. *Boundary-Layer Meteorology*, **91**, 81–107.

Medlyn BE, Loustau D, Delzon S (2002) Temperature response of parameters of a biochemically based model of photosynthesis. I. Seasonal changes in mature maritime pine (*Pinus pinaster* Ait.). *Plant, Cell and Environment*, **25**, 1155–1165.

Nikolov NT, Massman WJ, Schoettle AW (1995) Coupling biochemical and biophysical processes at the leaf level: an equilibrium photosynthesis model for leaves of C3 plants. *Ecological Modelling*, **80**, 205–235.

Norman JM (1979) Modeling the complete crop canopy. In: *Modifications of the Aerial Environment of Crops* (eds Barfield BJ, Gerber JF), pp. 249–277. American Society of Agricultural Engineers, St Joseph, Michigan.

Ogée J (2000) *Développement et applications du modèle MuSICA: étude des échanges gazeux d'eau et de carbone entre une pinède landaise et l'atmosphère*. PhD Thesis, Université Paul Sabatier – Toulouse III, Toulouse.

Ogée J, Brunet Y (2002) A forest floor model for heat and moisture including a litter layer. *Journal of Hydrology*, **255**, 212–233.

Oker-Blom P, Smolander H (1988) The ratio of shoot silhouette area to total needle area in Scots pine. *Forest Science*, **34** (4), 894–906.

Paw UKT (1987) Mathematical analysis of the operative temperature and energy budget. *Journal of Thermal Biology*, **12** (3), 227–233.

Pereira AR, Shaw RH (1977) A simulation of the effects of buoyancy on canopy flow. In: *13th American Meteorological Society Conference on Agricultural and Forest Meteorology*, Purdue University, West Lafayette, IN.

Porté A (1999) *Modélisation des effets du bilan hydrique sur la production primaire et la croissance d'un couvert de pins maritimes* (*Pinus pinaster Ait.*) *en lande humide*. PhD Thesis, Université d'Orsay – Paris XI, Orsay.

Porté A, Bosc A, Champion I *et al.* (2000) Estimating the foliage area of maritime pine (*Pinus pinaster* Aït.) branches and crowns with application to modelling the foliage area distribution in the crown. *Annals of Forest Science*, **57**, 73–86.

Porté A, Loustau D (1998) Variability of the photosynthetic characteristics of mature needles within the crown of a 25-year old *Pinus pinaster*. *Tree Physiology*, **18**, 223–232.

Porté A, Trichet P, Bert D *et al.* (2002) Allometric relationships for branch and tree woody biomass of maritime pine (*Pinus pinaster* Aït.). *Forest Ecology and Management*, **158**, 71–83.

Press WH, Teukolski SA, Vettering WT *et al.* (1992) *Numerical Recipes in Fortran 77*, 2nd edn. Cambridge University Press, Cambridge, UK.

de Pury DGG, Farquhar GD (1997) Simple scaling of photosynthesis from leaves to canopies without the errors of big-leaf models. *Plant, Cell and Environment*, **20**, 537–557.

Rasse DP, François L, Aubinet M *et al.* (2001) Modelling short-term CO_2 fluxes and long-term tree growth in temperate forests with ASPECTS. *Ecological Modelling*, **141**, 35–52.

Raupach MR (1989a) Applying Lagrangian fluid mechanics to infer scalar source distributions from concentration profiles in plant canopies. *Agricultural and Forest Meteorology*, **47**, 85–108.

Raupach MR (1989b) A practical Lagrangian method for relating scalar concentrations to source distributions in vegetation canopies. *Quarterly Journal of the Royal Meteorological Society*, **115**, 609–632.

Sellers PJ (1985) Canopy reflectance, photosynthesis and transpiration. *International Journal of Remote Sensing*, **6**(8), 1335–1372.

Shaw RH, den Hartog G, Neumann HH (1988) Influence of foliar density and thermal stability on profiles of Reynolds stress and turbulence intensity in a deciduous forest. *Boundary-Layer Meteorology*, **45**, 391–409.

Su H-B, Paw UKT, Shaw RH (1996) Development of a coupled leaf and canopy model for simulation of plant–atmosphere interaction. *Journal of Applied Meteorology*, **35**, 733–748.

Wang YP, Jarvis PG (1990) Influence of crown structural properties on PAR absorption, photosynthesis and transpiration in Sitka spruce: applications of a model (MAESTRO). *Tree Physiology*, **7**, 297–316.

Wang YP, Jarvis PJ (1993) Influence of shoot structure on the photosynthesis of Sitka spruce (Picea sitchensis). *Functional Ecology*, **7**, 433–451.

Wang K, Kellomäki S, Laitinen K (1995) Effects of needle age, long-term temperature and CO_2 treatments on the photosynthesis of Scots pine. *Tree Physiology*, **15**, 211–218.

Watanabe T, Mizutani K (1996) Model study on micrometeorological aspects of rainfall interception over an evergreen broad-leaved forest. *Agricultural and Forest Meteorology*, **80**, 195–214.

Whitehead D, Jarvis PJ, Whaning RH (1984) Stomatal conductance, transpiration and resistance to water uptake in a *Pinus sylvestris* spacing experiment. *Canadian Journal of Forest Research*, **14**, 692–700.

Whitehead D, Kelliher FM (1991) A canopy water balance model for a *Pinus radiata* stand before and after thinning. *Agricultural and Forest Meteorology*, **55**, 109–126.

Williams M, Rastetter EB, Fernandes DN *et al.* (1996) Modelling the soil–plant–atmosphere continuum in a Quercus-Acer stand at Harvard Forest: the regulation of stomatal conductance by light, nitrogen and soil/plant hydraulic properties. *Plant, Cell and Environment*, **19**, 911–927.

Willmott CJ (1981) On the validation of models. *Physical Geography*, **2**, 184–194.

Wilson KB, Baldocchi DD, Hanson PJ (2000) Spatial and seasonal variability of photosyntetic parameters and their relationship to leaf nitrogen in a deciduous forest. *Tree Physiology*, **20**, 565–578.

Wilson KB, Baldocchi DD, Hanson PJ (2001) Leaf age affects the seasonal pattern of photosynthetic capacity and net ecosystem exchange of carbon in a deciduous forest. *Plant, Cell and Environment*, **24**, 571–583.

Wilson K, Goldstein A, Falge E *et al.* (2002) Energy balance closure at FluxNet sites. *Agricultural and Forest Meteorology*, **113**, 223–243.

Wu J, Liu Y, Jelinski DE (2000) Effects of leaf area profiles and canopy stratification on simulated energy fluxes: the problem of vertical spatial scale. *Ecological Modelling*, **134**, 283–297.